

First-Principles Study on Electronic Properties of Low-Index ZnO Surfaces

J.H. ZHAO^{1,2,*}, E.J. HAN^{1,2}, T.M. LIU^{1,2} and W. ZENG^{1,2}

¹College of Materials Science and Engineering, Chongqing University, Chongqing 400030, P.R. China

²National Engineering Research Center for Magnesium Alloys, Chongqing University, Chongqing 400030, P.R. China

*Corresponding author: Fax: +86 023 65112611; Tel: +86 023 65112611; E-mail: jhzhao_cqu@163.com

(Received: 18 June 2011;

Accepted: 3 February 2012)

AJC-11030

The density functional theory plane-wave pseudopotential method was employed to study four low-index ZnO surfaces, which were (001), (100), (101) and (110) respectively. The structural parameters, band structures, density of states and the charge densities have been investigated. Present results show that the surfaces form the sequence (110) < (100) < (101) < (001) in order of increasing energy. The prediction that (110) is rather more stable. Both atoms displacements and the change of bond lengths after relaxing are observed. The changing values of (110) are the least, which is consistent with the prediction. The calculations of band structures and density of states suggest that valence bands of the four surfaces mainly consist of Zn 3d and O 2p orbitals and the conduction bands are mainly composed by O 2p states. Additionally, (110) has the narrowest band gap and the least charge density.

Key Words: First-principles, ZnO, Low-index surfaces, Electronic properties.

INTRODUCTION

In recent years, ZnO specific electronic and optical properties have received increasingly attention. The wide band gap and large exciton binding energy make it a promotive candidate for blue and ultraviolet light-emitting diodes¹⁻⁴. Until now, ZnO has been widely utilized in solar cells⁵, gas sensors⁶, liquid crystal display monitors⁷ and transparent high power electronic devices^{2,4}, etc. As we all know, regardless of ZnO applied in gas-sensing systems or fabrication of transparent thin-film transistors, the surface plays an indispensable role in understanding the mechanisms of surface chemical reaction and for the fabrication of high quality hetero- and homoepitaxial film with long-term stability⁸. As a result, the understanding of the physics and chemistry of ZnO surfaces is a topic of pronounced general interest and of course, also a necessary prerequisite for many technical applications⁹.

Presently, its surface have been extensively used as active catalysts and catalyst supports and intensively studied both experimentally and theoretically^{3,10-23}. Furthermore, it has received some attention in surface science²⁴⁻²⁸ for its role in the low-temperature synthesis of methanol⁸. In addition, its surface adsorption also have increasingly received interest in adsorption properties^{1,29,30}. Experimentally, Diebold *et al.*⁸ investigated the morphologies of all relevant low-index ZnO surfaces. The experiment indicated the Zn-terminated, c-oriented surfaces are characterized by a high roughness and

(100) orientation might be a good choice for growing ZnO films of superior quality because of the low surface energy. Nevertheless, it doesn't point detailed electronic structures of ZnO surfaces. Theoretically, semi-empirical and accurate density functional methods have been applied to study structures and electronic properties of atom or molecule adsorbed surfaces of ZnO. Zhi *et al.*¹ adopted first-principles calculations to study various surface structures in the absorption of Ag and Au atoms on wurtzite ZnO (001) surface. As a gas sensor device, its gas sensitivity has been detected. Spencer *et al.*²⁹ reviewed ZnO (10-10) and (2-1-10) surfaces' structure, properties and adsorption of N₂O. So far, (001) and (100) surfaces have become the subject of intensive works^{1,8,29} in past due to the reason that they have special better properties, which is thus investigated in this work.

Up to date, although many studies have investigated the physical and chemical properties of ZnO surfaces⁹, there is no detailed and systemic investigation on the structural parameters and associated electronic properties of ZnO surfaces. In this paper, we employed first-principles calculations to investigate the electronic structures on four low-index ZnO surfaces, that is, (001), (100), (101) and (110), respectively. In the initial step, we focused on the atomic and the electronic structures of ZnO surfaces to investigate the properties and for preparing high-performance of ZnO semiconductor materials. Besides, the work may give valuable messages for the study on structural and electronic properties of ZnO.

EXPERIMENTAL

It is well known that the most stable bulk ZnO belongs to the wurtzite structure (Fig. 1)³⁰. It has hexagonal symmetry $C_{6v}^4 - P6_3/mnm$ with lattice parameters $a = b = 3.25 \text{ \AA}$, $c = 5.21 \text{ \AA}$, $u = 0.345 \text{ \AA}^3$. ZnO is a triangular cone, edge length is shorter than bottom side and the bond length between central atom and top atom is slightly larger than central atom to the other three atoms on the taper surface. ZnO crystallizes in the wurtzite structure with each O^{2-} ion surrounded by a tetrahedron of four Zn^{2+} ions and *vice versa*. The structure lacks inversion symmetry and cutting the crystal perpendicular to the c-axis results in two structurally different surfaces⁸.

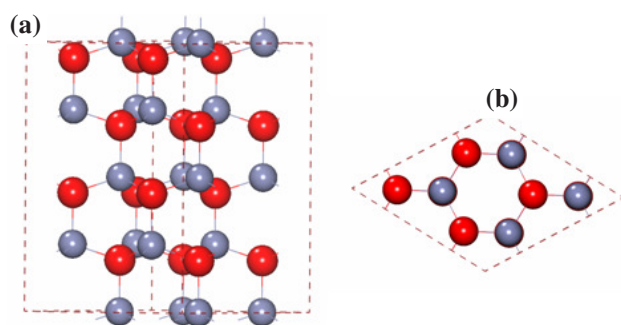


Fig. 1. ZnO wurtzite crystal structure; (a) side view (b) top view

In this study, calculation of the total energy was carried out using the Vienna *Ab initio* simulation package (VASP) code, within the framework of DFT³¹. The ultrasoft pseudo-potential was used for the electron-ion interactions and the Perdew-Burke-Ernzerhof formed of generalized gradient approximation (GGA)³² was employed to describe the exchange-correlation function. Generalized gradient approximation is chosen rather than the local density approximation since previous calculations have shown that this function is generally better at predicting the lattice parameters of ZnO³³. A cut-off energy of 450 eV was adopted to ensure energy convergence within 1-2 meV/atom³⁴. The task of geometry optimization is to improve the structural geometry to obtain more stable crystal structure through an iterative process. This process can minimize the total energy of the structure by adjusting atomic coordinates and cell parameters to make the following calculation more accurate. In all our calculations, no atoms are held fixed and all atoms are allowed to relax freely. The surface calculations were performed using a slab model with periodic boundary conditions¹². Slabs with increasing number of surface layers were cleaved from the bulk ZnO wurtzite structure, corresponding to (001), (100), (101) and (110) surfaces. As for the surface models, a vacuum region of 10 \AA is embedded along the surface normal to avoid unwanted interaction between the slab and its period images. The established (001), (100), (101) and (110) surface models are schematically shown in Fig. 2. In order to make sure that the surface supercell parameters were calculated accurately, we performed a full geometry optimization of the four ZnO surfaces and then calculated the four electronic structures, respectively.

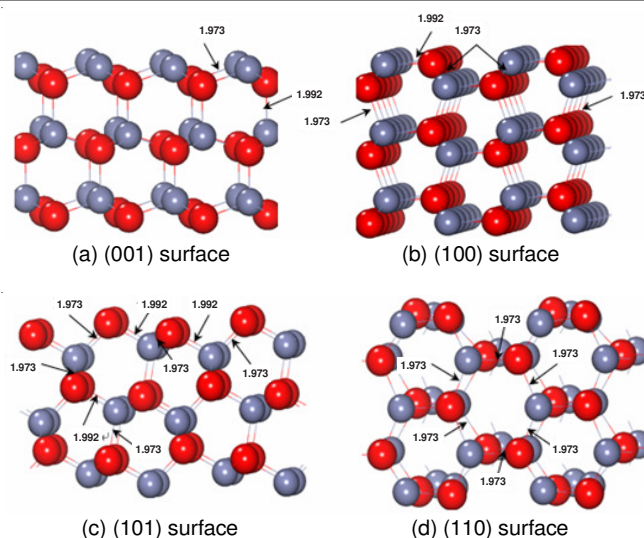


Fig. 2. Schematic models of the low-index unrelaxed surfaces of wurtzite ZnO: (a) (001); (b) (100); (c) (101) and (d) (110). Arrows and the corresponding values show bond lengths between oxygen atoms and Zinc atoms in different directions. Red and gray spheres show O and Zn ions, respectively

RESULTS AND DISCUSSION

Relaxed slab Models

Surface energies: The investigation was started from the surface structure by using the optimized lattice parameters, as (100) surface for example, yielding $a = 3.206 \text{ \AA}$, $c = 5.205 \text{ \AA}$, in general agreement with theoretical data, of $a = 3.268 \text{ \AA}$, $c = 5.233 \text{ \AA}$, respectively²⁹. They are also consistent with previous experimental studies³⁵.

The surface energy E_{sur} is calculated as follows³⁶:

$$E_{\text{sur}} = \frac{1}{2A} \left(E_{\text{slab}} - \frac{N_{\text{slab}}}{N_{\text{bulk}}} E_{\text{bulk}} \right)$$

where, E_{slab} and E_{bulk} are the total energies of the surface slab and the bulk unit cell, respectively. Here we neglect finite temperature contributions to the surface free energy³⁷. E_{slab} and E_{bulk} are the number of formula units contained in the slab and the bulk supercell, respectively. A is the area of the surface cell.

The calculated surface energies are shown in Table-1. One can easily find that, in order of increasing energy, the surfaces form the sequence (110) < (100) < (101) < (001). That is to say (110) is the most stable and (001) is the least stable of the four surfaces. The prediction that (110) is the most stable surface generally agrees with earlier experimental and theoretical indications. However, Diebold *et al.*⁸ points that ZnO (100) surface shows high stability, small roughness and well-defined terrace structure allowing itself for the growth of high-quality films. So it believes that (100) surface is better than the other surfaces it observed, including (110) surface, where the different view exists. But considering other studies, there is no obvious disagreement, as energies of the two surfaces are very close with previous reports^{38,39}. It's worth mentioning here that the absolute values of the surface energies derived from DFT calculations depend on the approximations that are used⁴⁰. In other words, different function, such as B3LYP

functional, local density approximation or generalized gradient approximation, employed in the various calculations is likely to obtain different results. But only results founded by using the same approximations should be compared.

TABLE-1
CALCULATED SURFACE ENERGIES
OF THE FOUR ZnO SURFACES

ZnO surfaces	$E_{\text{sur}}(\text{J/m}^2)$
(001)	3.22
(100)	2.54
(101)	2.62
(110)	2.24

Bond length: The optimized geometry of the minimum energy structures for the four ZnO surfaces are shown in Fig. 3, with the calculated bond length after relaxation, also including the changing values. A positive value indicates expansion, while a negative value indicates contraction. Because the dimmer bond length is strongly dependent on the choice of the exchange-correlation potential, the calculated values may be slightly different from previous works.

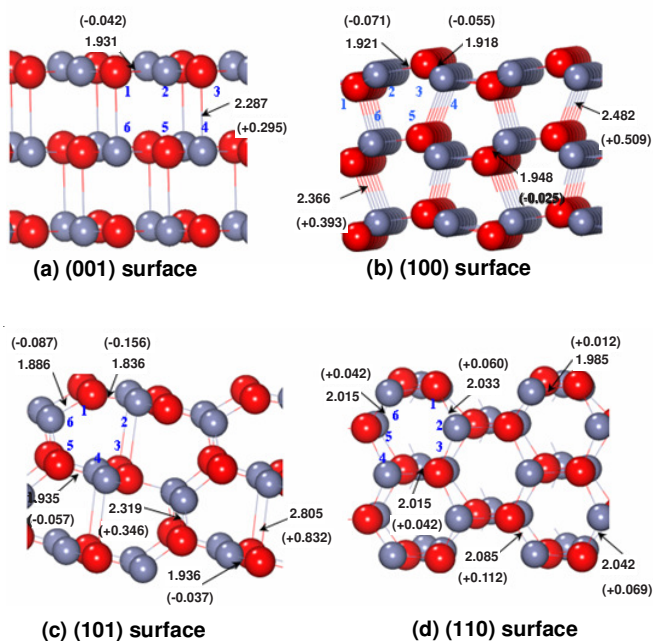


Fig. 3. Relaxed ionic positions at the (a) (001), (b) (100), (c) (101) and (d) (110) surface, respectively. Arrows and values (\AA) represent bond lengths after relaxation and the changing magnitudes are marked (in parentheses)

We can easily draw the following conclusions by combining Figs. 2 and 3: (a) The bond lengths of the four surfaces vary without rigorous regularity after optimization and each variation is unequal to the others; (b) For the first three surfaces, some bond lengths increase whereas others decrease, however, the bond lengths of the fourth surface only increase without reducing; (c) The bond lengths of outermost atoms are inclined to be diminished, which agrees well with previous studies; (d) The bond lengths for (110) surface have the minimum variation compared with relative violent changes on other three surfaces.

Generally speaking, the change of (001) (Fig. 2a) is rather balanced, but the increment is much greater than the reduction. The change for (100) surface resemble quite closely those on (001) and a larger obvious increment value ups to 0.509\AA . As to (101) surface, the most striking feature is the largest changed value reaching 0.832\AA . The bond lengths on (110) surface all increase in a small scope, which is different from the other three surfaces. It is coincided with the preceding calculation result that the energy of (110) surface is the lowest one, illustrating the (110) surface is comparatively steady.

Band structure and density of states: To further investigate the electronic properties of the four surfaces, we present band structure in Fig. 4, with the Fermi energy being 0 eV on the energy axis. And the total density of states and partial density of states of the system are shown in Fig. 5.

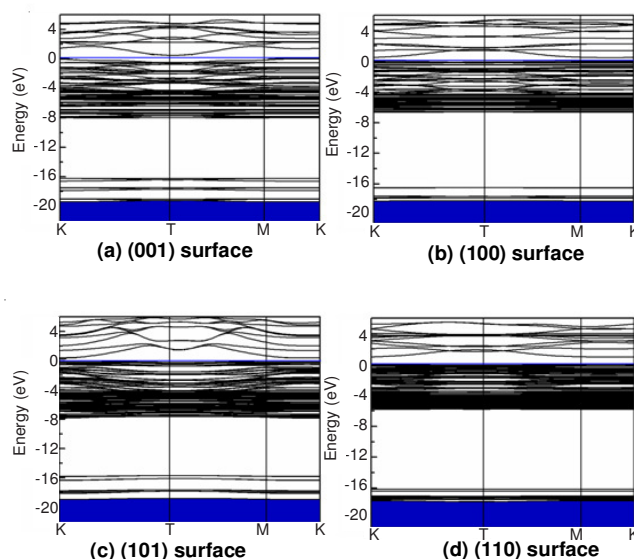


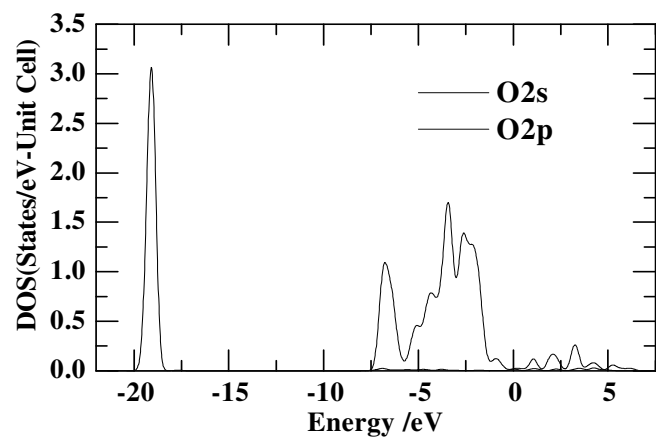
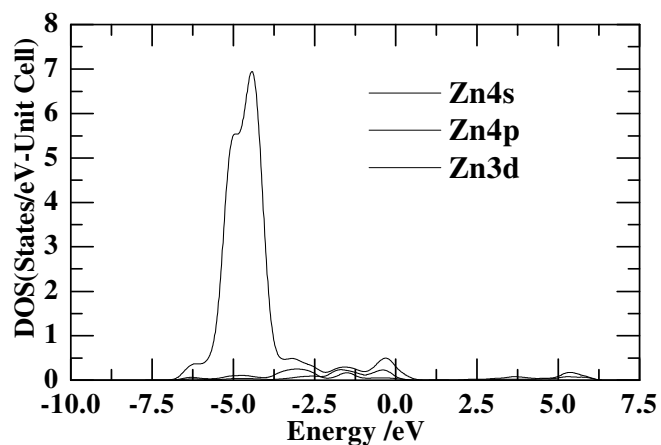
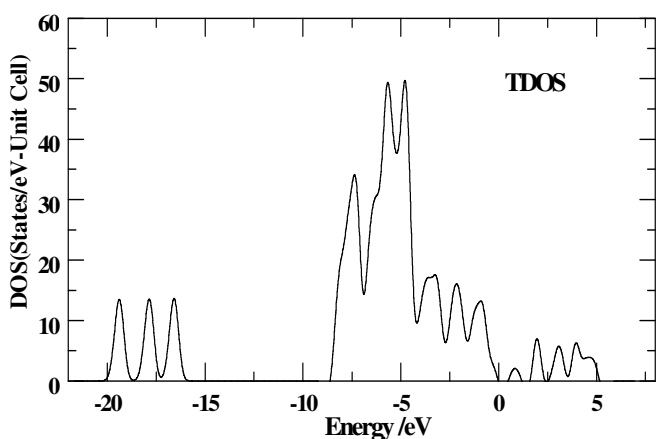
Fig. 4. Band structures of the four ZnO surfaces: (a) (001), (b) (100), (c) (101) and (d) (110) surface, respectively

Generally speaking, from Fig. 4, the calculated band gaps are 0.49 , 0.74 , 0.322 and 0.814 eV , corresponding to (001), (100), (101) and (110) surface, respectively, which is lower than the experimental values. This is regarded as a general problem of the DFT calculation²⁴. For the clean ZnO (001) surface, Zhi *et al.*¹ obtain the surface band gap value of 0.343 eV , which is smaller than 0.49 eV . However, the DFT calculations are still able to predict the trend of band gap⁴¹. Among the four band gaps, we can easily know the biggest one is (110) and the smallest one is (001).

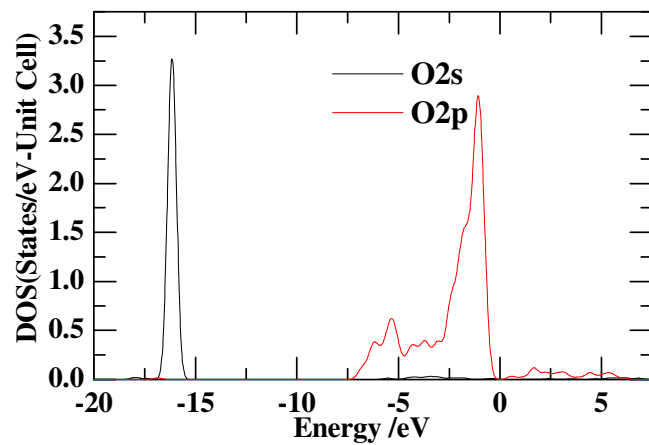
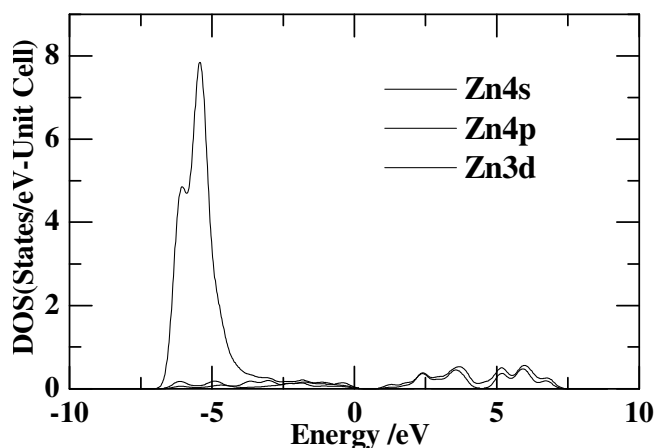
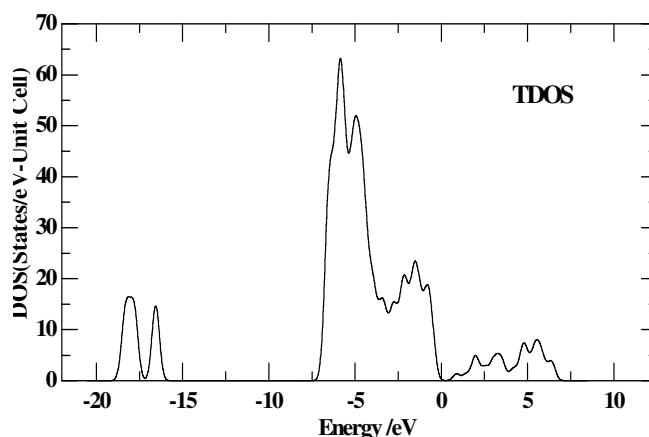
It can be seen from Fig. 5a that the valence band (VB) between -0.01 and -9.2 eV is mainly from the Zn 3d and O 2p orbitals with a small portion from Zn 4s and Zn 4p, while the major contributions to the lower valence band between -20.6 and -15.6 eV is originated mainly from O 2s orbital. We can also find that there is hybridization between Zn 3d and O 2p orbital in the valence band. The conduction band (CB) between 0.48 and 5.88 eV are mainly contributed by O 2p orbital, mixed with some Zn 4s and Zn 4p states. Though the composition of valence band and conduction band of the other three surfaces, from Fig. 5(b-d), are very similar to what we have mentioned for (001) surface, bands regions and positions are different.

For (100) surface, the lowest band of valence band is from -19.45 to -15.54 eV and the top of valence band is from -7.72 to -0.11 eV. The band gap is from -0.11 to 0.63 eV and the conduction band is from 0.63 to 7.25 eV. Similarly, the regions of the lowest and highest valence band, band gap and conduction band for (101) surface are (-21.32 eV, -15.97 eV) and (-9.91 eV, -0.022 eV), (-0.022 eV, 0.3 eV) and (0.3 eV, 5.48 eV), respectively. Then the values for (110) surface are (-19.04 eV, -15.69 eV), (-7.23 eV, -0.004 eV), (-0.004 eV, 0.81 eV) and (0.81 eV, 5.87 eV), respectively.

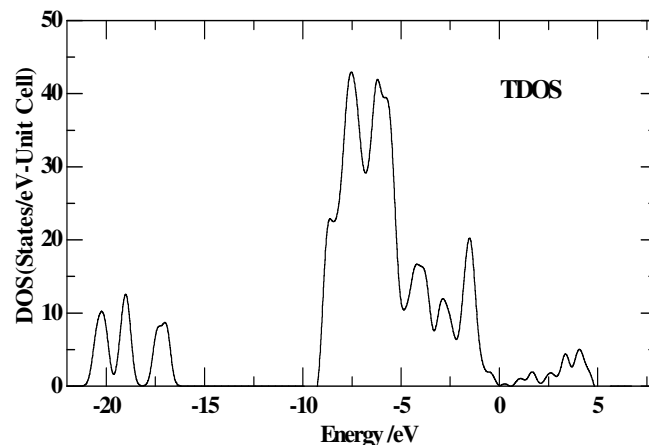
The analysis of the atomic orbital contribution for the valence band maximum (VBM) of all the four surfaces show that the valence band maximum is mainly occupied by the Zn 3d and O 2p orbital. But the positions of the peak for Zn 3d and O 2p states are slightly different from Fig. 5.

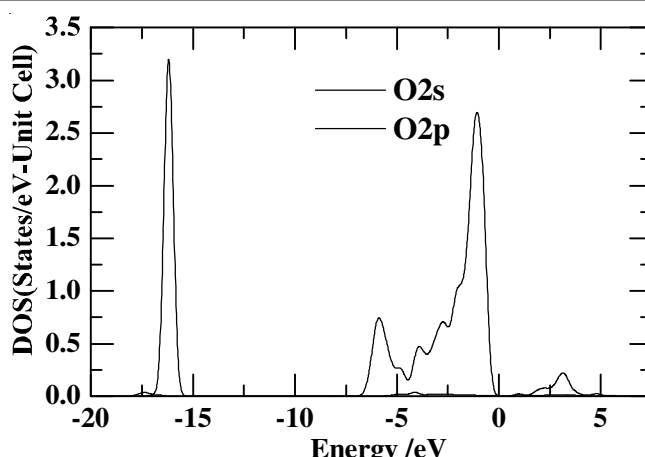
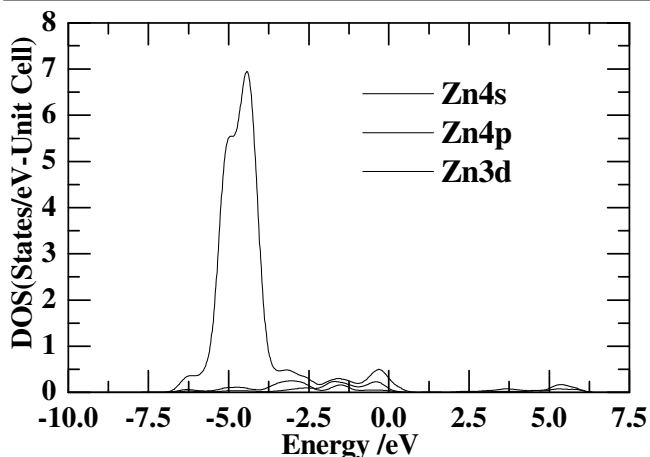


(a) (001) surface

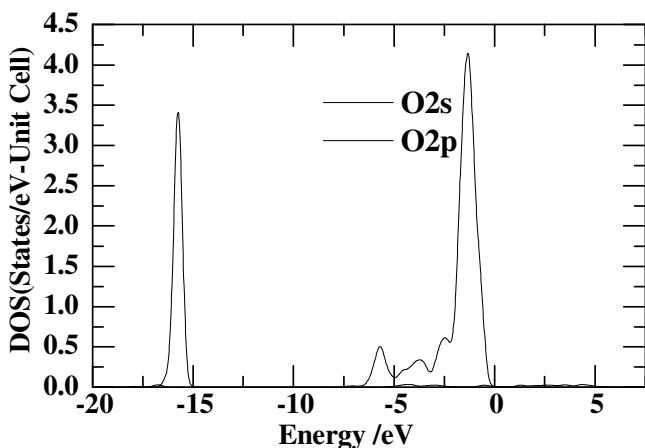


(b) (100) surface

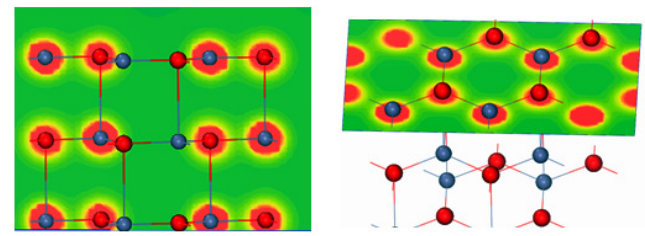
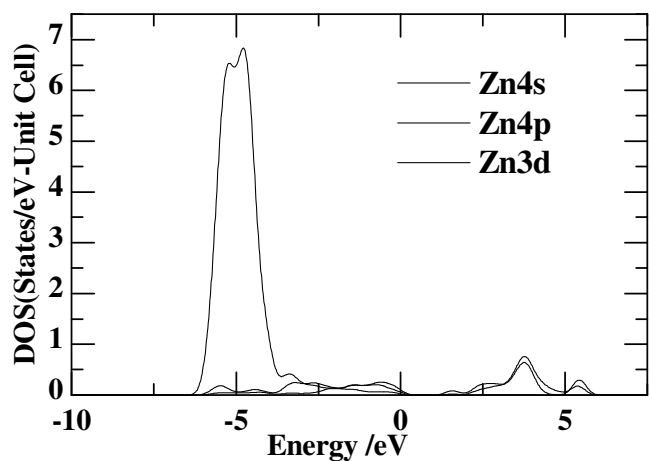
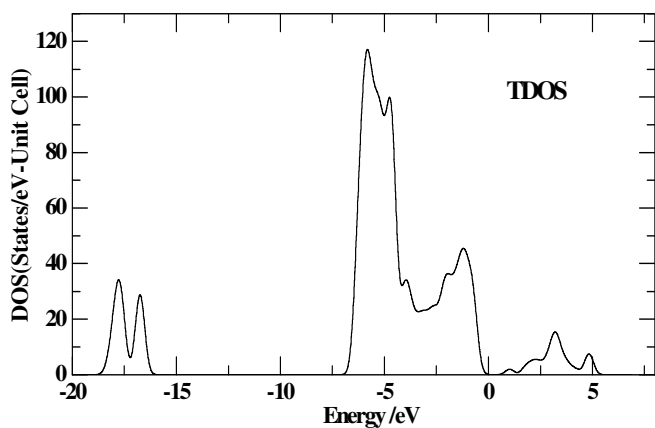




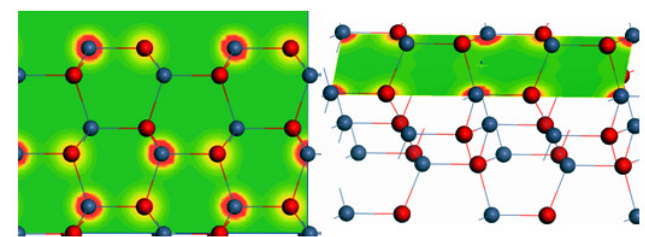
(d) (110) surface



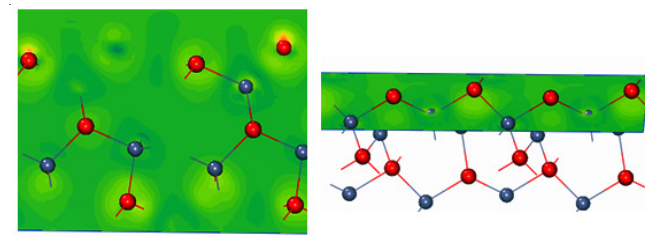
(c) (101) surface



(a) (001) surface



(b) (100) surface



(c) (101) surface

Fig. 5. Density of states and partial density of states of ZnO surfaces: (a) (001), (b) (100), (c) (101) and (d) (110) surface, respectively

Charge density: To further investigate the electronic properties of ZnO surfaces, we present the charge density in Fig. 6. From Fig. 6a, we find that charge density around Zn atoms are nearly the same as O atoms. But as for (100) surface (Fig. 6b), charge density around Zn atoms are stronger than O atoms. To (110) surface (Fig. 6d), this phenomenon becomes more obvious. Interestingly, charge density of (101) surface (Fig. 6c) is very weak. So it is the least charge density among the four surfaces. It is worth noting that the band gap of (101) surface is also the smallest one. Thus we predict that band gap may have some thing to do with charge transfer.

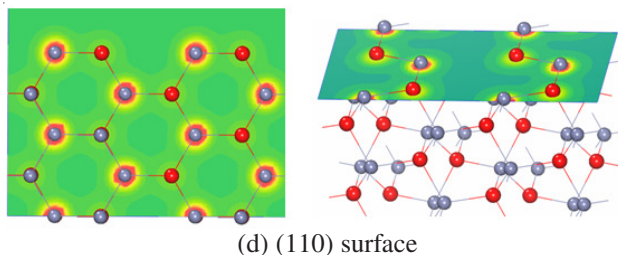


Fig. 6. Electron density maps of top and side view of ZnO (a) (001) surface, (b) (100) surface, (c) (101) surface and (d) (110) surface, respectively

Conclusion

We have performed a first-principles study of the four low-index ZnO surfaces. The structural and electronic and energy band properties have been investigated. The conclusion can be summarized as follows: (1) We first optimize the four low-index ZnO surfaces. At the same time, we obtain optimized structural parameters, surface energies, bond lengths and atoms displacements after relaxation; (2) The results of the calculated atoms relaxations generally agree with the theoretical and experimental studies. (110) has the lowest surface energy and the smallest relaxations. These findings indicate that (110) is the most stable surface among the four investigated surfaces; (3) The calculation of band gaps and density of states point that the valence bands of the four surfaces mainly consist of Zn 3d and O 2p orbitals and the conduction bands are mainly composed by O 2p state. What the differences are regions and positions of these orbitals and the contribution of other states; (4) From the calculation of charge density, present study shows that the charge density of (001) and (100) surface is more than the other two surfaces. The lowest charge density of (101) surface may affect the width of band gap.

ACKNOWLEDGEMENTS

This work was supported in part by the Fundamental Research Funds for the Central Universities (CDJXS10131154) and a Distinguished PhD award from Ministry of Education of China. One of the authors (Zeng Wen) thanks the Chinese Scholarship Council (CSC) project (LJC20093012) for scholarship support.

REFERENCES

- Z. Yang and S.J. Xiong, *Surf. Sci.*, **605**, 40 (2010).
- D.M. Bagnall, Y.F. Chen, Z. Zhu, T. Yao, S. Koyama, M.Y. Shen and T. Goto, *Appl. Phys. Lett.*, **70**, 2230 (1997).
- J. Yoshihara, J.M. Campbell and C.T. Campbell, *Surf. Sci.*, **406**, 235 (1998).
- S.J. Pearton, D.P. Norton, K. Ip, Y.W. Heo and T.S. Steiner, *J. Vac. Sci. Technol. B*, **22**, 932 (2004).
- M. Bar, J. Reichardt, A. Grimm, I. Kotschau, I. Lauermann, K. Rahne, S. Sokoll, M.C. Lux-Steiner, C.H. Fischer, L. Weinhardt, E. Umbach, C. Heske, C. Jung, T.P. Niesen and S. Visbeck, *J. Appl. Phys.*, **98**, 053702 (2005).
- H.B. Huo and Z.X. Fan, *Acta Optica Sinica*, **18**, 1676 (1998).
- H.J. Kim, H.N. Lee, J.C. Park and W.G. Lee, *Curr. Appl. Phys.*, **2**, 451 (2002).
- U. Diebold, L.V. Koplitz and O. Dulub, *Appl. Surf. Sci.*, **237**, 336 (2004).
- C. Wöll, *Prog. Surf. Sci.*, **82**, 55 (2007).
- K.H. Ernst, A. Ludviksson, R. Zhang, J. Yosihara and C.T. Campbell, *Phys. Rev. B*, **47**, 13782 (1993).
- B. Meyer and D. Marx, *Phys. Rev. B*, **69**, 035403 (2004).
- V. Ney, S. Ye, T. Kammermeier, A. Ney, H. Zhou, J. Fallert, H. Kalt, F.Y. Lo, A. Melnikov and A.D. Wieck, *J. Appl. Phys.*, **104**, 083904 (2008).
- J. Wang, B. Hokkanen and U. Burghaus, *Surf. Sci.*, **577**, 158 (2005).
- R.G.S. Pala and H. Metiu, *J. Catal.*, **254**, 325 (2008).
- S.T. Bromley, S.A. French, A.A. Sokol, C.R.A. Catlow and P. Sherwood, *J. Phys. Chem. B*, **107**, 7045 (2003).
- X.Q. Dai, H.J. Yan, J.L. Wang, Y.M. Liu, Z.X. Yang and M.H. Xie, *J. Phys. Condens. Matter*, **20**, 095002 (2008).
- E.Z. Liu and J.Z. Jiang, *J. Phys. Chem. C*, **113**, 16116 (2009).
- S.A. French, A.A. Sokol, C.R.A. Catlow and P. Sherwood, *J. Phys. Chem. C*, **112**, 19 (2008).
- P. Lazcano, M. Batzill, U. Diebold and P. Haberle, *Phys. Rev. B*, **77**, 035435 (2008).
- N.S. Phala, G. Klatt, E. van Steen, S.A. French, A.A. Sokol and C.R.A. Catlow, *Phys. Chem. Chem. Phys.*, **7**, 2440 (2005).
- J. Hu, W.P. Guo, X.R. Shi, B.R. Li and J.G. Wang, *J. Phys. Chem. C*, **113**, 7227 (2009).
- P. Persson and L. Ojamäe, *Chem. Phys. Lett.*, **321**, 302 (2000).
- L.V. Koplitz, O. Dulub and U. Diebold, *J. Phys. Chem. B*, **107**, 10583 (2003).
- G. Thornton, S. Crook and Z. Chang, *Surf. Sci.*, **415**, 122 (1998).
- V. Staemmler, K. Fink, B. Meyer, D. Marx, M. Kunat, S.G. Girol, U. Burghaus and C. Wöll, *Phys. Rev. Lett.*, **90**, 106102 (2003).
- A. Wander, F. Schedin, P. Steadman, A. Norris, R. McGrath, T.S. Turner, G. Thornton and N.M. Harrison, *Phys. Rev. Lett.*, **86**, 3811 (2001).
- T.M. Parker, N.G. Condon, R. Lindsay, F.M. Leibsle and G. Thornton, *Surf. Sci.*, **415**, L1046 (1998).
- M. Kunat, S.G. Girol, T. Becker, U. Burghaus and C. Wöll, *Phys. Rev. B*, **66**, 081402 (2002).
- M.J.S. Spencer, K.W.J. Wong and I. Yarovsky, *Mater. Chem. Phys.*, **119**, 505 (2010).
- J. Oviedo and M.J. Gillan, *Surf. Sci.*, **463**, 93 (2000).
- G. Kresse and J. Furthmüller, *Phys. Rev. B*, **54**, 11169 (1996).
- J. Goniakowski, J.M. Holender, L.N. Kantorovich, M.J. Gillan and J.A. White, *Phys. Rev. B*, **53**, 957 (1996).
- C.L. Phillips and P.D. Bristowe, *Surf. Sci.*, **605**, 450 (2011).
- W. Zeng, T.M. Liu and X.F. Lei, *Physica B*, **405**, 564 (2010).
- C.B. Duke, R.J. Meyer, A. Paton and P. Mark, *Phys. Rev. B*, **18**, 4225 (1978).
- A. Arya and E.A. Carter, *J. Chem. Phys.*, **118**, 8982 (2003).
- Q.L. Chen, C.Q. Tang and G. Zheng, *Physica B*, **404**, 1074 (2009).
- B. Meyer and D. Marx, *Phys. Rev. B*, **67**, 035403 (2003).
- G. Kresse, *Private communication*
- A.E. Mattsson and D.R. Jennison, *Surf. Sci.*, **520**, L611 (2002).
- J. Kang, Y. Zhang, Y.H. Wen, J.C. Zheng and Z.Z. Zhu, *Phys. Lett. A*, **374**, 1054 (2010).